Further Details on Computational Experiments

Shengnan Shu
Department of Logistics and Maritime Studies, Hong Kong Polytechnic University, shengnan.shu@connect.polyu.hk
Zhou Xu
Department of Logistics and Maritime Studies, Hong Kong Polytechnic University, lgtzx@polyu.edu.hk
Jin Qi
Department of Industrial Engineering and Decision Analytics, Hong Kong University of Science and Technology, jinqi@ust.hk

1. Instance Generation for Computational Experiments

For our computational experiments, we generated instances of the robust CTSNDP based on the seven instance classes (named R4-R10) of the fixed-charge capacitated multi-commodity network design (CMND) problem available in the literature Ghamlouche et al. (2003). These classes of CMND instances have been utilized in previous studies to generate test instances for various stochastic capacitated fixed charge network design problems (see, for example, Crainic et al. 2011, Sarayloo et al. 2021a,b). Their sizes are comparable to those in previous studies on SNDP under uncertainties (Wang and Qi 2020, Lanza et al. 2021).

The sizes of the node set $\mathcal{N}$, arc set $\mathcal{A}$, and commodity set $\mathcal{K}$ vary from 10 to 20, from 60 to 120, and from 10 to 50, respectively, among instances belonging to different classes. These instances are referred to as "untimed" instances, as they do not have any temporal attributes such as travel times of arcs, or earliest available times and due times of commodities. Moreover, each of these instance classes consists of five networks with different "ratio" indices valued from 1, 3, 5, 7, to 9. These index values indicate different combinations of ratios of fixed cost to variable cost and total demand to total network capacity, with values of (0.01, 1), (0.1, 1), (0.05, 2), (0.01, 8), and (0.1, 8), respectively.

To obtain "timed" instances for each of the 7 classes of the CMND problem, we followed an approach similar to that presented in Boland et al. (2017) to generate fixed costs and time attributes of the CTSNDP. First, for each arc $(i, j) \in \mathcal{A}$, we set the nominal value of travel time (in minutes) $\overline{\tau}_{ij}$ to be proportional to its fixed cost f_{ij} by setting $\overline{\tau}_{ij} = f_{ij}/0.55$, as in Boland et al. (2017). This

is based on the same premise that f_{ij} represents the transportation cost for carriers that spend 0.55 cents per mile, and that their trucks travel at 60 miles per hour.

Next, for each commodity $k \in \mathcal{K}$, we followed a normal distribution to randomly generate the available time e^k. Let $\mathscr{L}_k$ denote the length of the shortest-time path from origin o^k to destination d^k for commodity k in the flat network under the nominal travel times $\overline{\boldsymbol{\tau}}$. We then set the due time l^k of each commodity $k \in \mathcal{K}$ by $l^k = e^k + \mathscr{L}_k + \mathscr{F}_k$. Here, the parameter $\mathscr{F}_k \geq 0$ represents the time flexibility for the delivery of commodity k, which we also set randomly using a normal distribution. We used the same normal distribution to generate the available times e^k for all instances, but used two different normal distributions to generate $\mathscr{F}_k$ for instances of high and low time flexibility, respectively. Consequently, we had two combinations of normal distributions to generate commodities' available times and time flexibility. The detailed settings of these normal distributions are described in Table 1.1, where $\mathscr{L}$ denotes the average of $\mathscr{L}_k$ over all $k \in \mathcal{K}$.

Table 1.1 Detail setting of the normal distributions used for generating "timed" instances.

Normal Distribution	Mean(μ)	Standard Deviation(σ)
For generating e_k	$\mathscr{L}$	$\frac{1}{6}\mathscr{L}$
For generating $\mathscr{F}_k$	$\frac{1}{2}\mathscr{L}$	$\frac{1}{6} \cdot \frac{1}{2}\mathscr{L}$
	$\frac{1}{4}\mathscr{L}$	$\frac{1}{6} \cdot \frac{1}{4}\mathscr{L}$

For each "timed" instance obtained, we then generated unit in-storage holding costs and unit delay penalties for the commodities. We set the per-unit-of-demand-and-time in-storage holding cost h^k for each commodity $k \in \mathcal{K}$ to be proportional to its cheapest per-unit-of-time per-unit-of-flow cost, i.e., $h^k = 0.5 \min_{a \in \mathcal{A}}\{(c_a^k + f_a/u_a)/\overline{\tau}_a\}$ where $\overline{\tau}_a$ is the nominal value of the travel time generated. Inspired by Lanza et al. (2021), for each commodity $k \in \mathcal{K}$, we set its penalty g^k per unit of time for the delay to be twice the most expensive per-unit-of-time transportation cost for it to pass through an arc, i.e., $g^k = 2 \cdot \max_{a \in \mathcal{A}}\{(c_a^k \cdot q^k + f_a \lceil q^k/u_a \rceil)/\overline{\tau}_a\}$.

Moreover, to characterize travel time uncertainty, we generated the maximum deviation $\hat{\tau}_{ij}$ of the travel time for each arc $(i,j) \in \mathcal{A}$ by setting $\hat{\tau}_{ij} = \hat{\mu}_{ij}\overline{\tau}_{ij}$. Here, $\overline{\tau}_{ij}$ is the nominal value of the travel time generated, and $\hat{\mu}_{ij}$ is a coefficient randomly selected from 0.1 to 0.5.

For each network in each problem class, we randomly generated 3 instances for each combination of the distributions for commodities' available time and time flexibility. As a result, we obtained $5 \times 2 \times 3 = 30$ test instances for each of the 7 instance classes, and thus obtained $7 \times 30 = 210$ test instances in total.

In our second set of experiments, under different values of Γ and $\mathcal{Z}$, we need to evaluate the worst-case and average total costs of solutions obtained from models RO, RS and SP over randomly generated scenarios for instances in class R7. For each of the 30 instances in class R7, we generated 200 scenarios at random to create the set Π for model SP and model MM. To generate each scenario $\boldsymbol{\delta}$, we drew each of the realization of δ_{ijr} for $(i,j) \in \mathcal{A}$ and $r \in \{1,2,...,|\mathcal{K}|\}$ uniformly from the set $\{-1, -(\hat{\tau}_{ij}-1)/\hat{\tau}_{ij}, -(\hat{\tau}_{ij}-2)/\hat{\tau}_{ij}, \cdots, -1/\hat{\tau}_{ij}, 0, 1/\hat{\tau}_{ij}, \cdots, (\hat{\tau}_{ij}-1)/\hat{\tau}_{ij}, 1\}$.

2. Additional Computational Results

In this section, additional computational results are reported.

2.1. Details on Performance of RO-C&CG and RS-C&CG

Table 2.1 below presents the computational performances of RO-C&CG and RS-C&CG across instances with different cost and time attributes. As mentioned in Section 1, each CTSNDP instance origins from an untimed instance with a "ratio" index. The "ratio" index is valued from 1, 3, 5, 7, to 9, indicating combinations of ratios of fixed cost to variable cost ratio and total demand to total network capacity as (0.01, 1), (0.1, 1), (0.05, 2), (0.01, 8), and (0.1, 8), respectively. Moreover, each instance is associated with time flexibility parameters $\mathscr{F}_k$ for $k \in \mathcal{K}$, which follow a normal distribution with its mean equal to $\mathscr{L}/2$ or $\mathscr{L}/4$.

Accordingly, we regrouped the 210 CTSNDP instances into ten groups, according to their "ratio" indices and their means of time flexibility. In Table 2.1, for each instance group and each C&CG algorithm, we report the average optimality gap in column g% (defined as the percentage gap between the best upper and lower bounds found), the average computational time in CPU seconds in column T for C&CG algorithms for RO and RS. Moreover, we present the number of required directed shipping services in column #service, the percentage of services consolidating two or more commodities in column cons%, along with the flow cost and the fixed cost, for the final solution obtained by DO, RO-C&CG, and RS-C&CG.

Table 2.1 Details on Performance of RO-C&CG and RS-C&CG Algorithms

Ratio Index	Time Flexibility	DO				RO-C&CG						RS-C&CG					
		#service	cons%	flow cost	fixed cost	g%	T	#service	cons%	flow cost	fixed cost	g%	T	#service	cons%	flow cost	fixed cost
1	$\frac{1}{2}\mathscr{L}$	35.7	21.9	128893.0	30898.0	0.0	517.8	38.4	19.4	139567.3	30646.0	0.0	98.5	37.3	18.6	135181.1	30614.05
	$\frac{1}{4}\mathscr{L}$	39.2	16.3	143799.1	31009.6	0.0	12.6	41.5	13.0	146870.3	32109.7	0.0	15.9	41.2	13.3	146527.6	32229.33
3	$\frac{1}{2}\mathscr{L}$	33.2	36.2	153720.3	237499.5	0.1	3107.0	34.8	32.0	157323.2	248703.6	1.8	4289.7	34.7	31.4	158152.8	247637.9
	$\frac{1}{4}\mathscr{L}$	38.6	22.6	155527.2	284157.8	0.0	6.9	40.0	19.9	158075.1	293721.8	0.0	18.9	40.1	19.9	157175.0	293983.2
5	$\frac{1}{2}\mathscr{L}$	36.4	26.4	142456.7	151308.8	0.0	1631.9	38.5	22.0	148912.2	161119.5	0.4	3590.4	37.8	22.9	145256.7	158199.7
	$\frac{1}{4}\mathscr{L}$	40.3	16.7	148844.3	171846.1	0.0	12.3	42.5	13.5	153913.7	178427.3	0.0	29.1	42.0	14.1	152576.6	177666.7
7	$\frac{1}{2}\mathscr{L}$	40.7	12.2	134996.0	75388.3	0.0	62.1	42.7	10.6	141932.9	78952.0	0.0	192.2	42.3	9.6	137430.2	79375.62
	$\frac{1}{4}\mathscr{L}$	42.3	9.7	144741.9	81155.2	0.0	13.8	44.1	7.6	148991.5	83608.5	0.0	5.9	43.6	7.7	146458.5	83101.33
9	$\frac{1}{2}\mathscr{L}$	38.9	20.6	148237.5	505474.2	0.0	619.7	41.2	16.7	153456.0	531341.4	0.0	126.2	40.7	16.9	151853.1	522618.6
	$\frac{1}{4}\mathscr{L}$	42.7	12.3	152407.3	571584.3	0.0	3.9	43.9	9.9	154568.5	583166.0	0.0	11.8	43.7	9.6	153090.0	585582.5

From the results in Table 2.1 we can obtain the following insights. First, it can be seen that instances with greater time flexibility are more difficult to solve, especially when the ratio of fixed cost to variable cost and the ratio of total demand to total network capacity are both moderately large. Second, compared to the optimal deterministic solutions, robust solutions typically require more directed shipping services but fewer consolidations, thereby incurring higher transportation costs. Third, robust solutions often exhibit both higher average flow costs and fixed costs, resulting in higher total transportation costs. However, this trend does not always hold, since for certain instances, the flow costs or fixed costs of robust solutions may be lower than those of the optimal deterministic solutions.

2.2. Nominal Performance of Robust Solutions

We conducted additional computational experiments across 30 instances of class R7 to evaluate the performance of the robust solutions obtained from models RO and RS under the nominal scenario. For each instance in R7, we used RO-C&CG to solve model RO for each uncertainty budget $\Gamma \in \{1, 2, ..., 10\}$, and used RS-C&CG to solve model RS for each cost target $\mathcal{Z} = \lceil (1 + \mu_z) \cdot \mathcal{Z}_0 \rceil$ with $\mu_z \in \{0.02, 0.04, ..., 0.2\}$, where $\mathcal{Z}_0$ is set as the optimal objective value of model DO. For each robust solution obtained, we computed the total cost of its first-stage solution in the nominal scenario. We then solved model DO to obtain the minimum achievable total cost for the nominal scenario.

The results are presented in Figure 1, where the total cost along the vertical axis is the mean across all instances in R7. It can be seen that robust solutions typically exhibit inferior nominal performance compared to the optimal deterministic solution, since they prioritize the optimization of worst-case performance. However, solutions obtained from model RS exhibit better overall performance in the nominal scenario than those from model RO. This is because the robust optimization approach focuses exclusively on the worst-case total cost within the budget of uncertainty Γ, whereas model RS is solved within a specified acceptable cost loss relative to the nominal optimal solution under the nominal scenario, denoted as $\mathcal{Z} - \mathcal{Z}_0$. Moreover, it can be seen

Figure 1 **Total costs in nominal scenario**

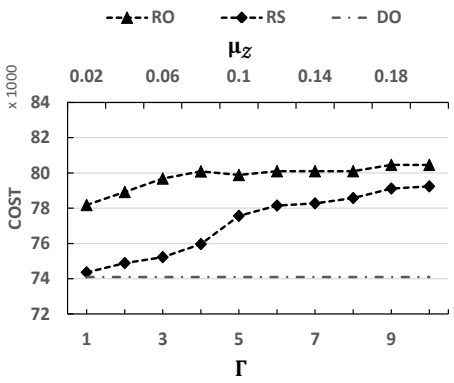

that when μ_z increases, the total nominal cost of the solutions from model RS gradually increases. In contrast, the total nominal cost of solutions obtained from model RO does not show a strictly monotonically increasing trend as Γ increases. This suggests that the cost target $\mathcal{Z}$ is more effective in controlling the price of robustness for robust solutions in terms of their performance loss in the nominal scenario.

2.3. Results for Large Instances

We followed the method described in Section 1 to generate 150 large CTSNDP instances from five classes (R11-R15) of the fixed-charge capacitated multi-commodity network design (CMND) problem in Ghamlouche et al. (2003), with each class containing 30 instances. For these large CTSPND instances, the number of nodes $|\mathcal{N}|$, the number of arcs $|\mathcal{A}|$, and the number of commodities $|\mathcal{K}|$ are presented in Table 2.2. For each of these large instances, we solved the deterministic model DO using the Gurobi solver within an 8-hour time limit, and set its final objective value as the cost target $\mathcal{Z}_0$ for RS-C&CG. The average optimality gap (g%) and computational time in CPU seconds (T) of model DO are presented in Table 2.2. Moreover, we set the uncertainty budget Γ of model RO and the cost target $\mathcal{Z}$ of model RS to $\lceil 0.05 \cdot |\mathcal{K}| \rceil$ and $\lceil (1+0.05) \cdot \mathcal{Z}_0 \rceil$, respectively.

The computational results are detailed in Table 2.2, including the percentage of instances solved optimally (opt%), the average optimality gap (g%), and the average computational time in CPU seconds (T) for each C&CG algorithm across different instance classes. Additionally, we present the mean and maximum of improvement ratio against the obtained deterministic solution of model DO, with respect to the objective value of the corresponding robust model, in columns under Im%. Specifically, the improvement ratio for each instance is computed by $\frac{C_{DO}-\text{UB}}{C_{DO}}$, where C_{DO} represents the objective value of the corresponding robust model achieved by the obtained deterministic solution and UB represents the best upper bound value found for the corresponding robust model.

Table 2.2 Computational Performance of RO-C&CG and RS-C&CG Algorithms over Large Instances

class	$\|\mathcal{N}\|$	$\|\mathcal{A}\|$	$\|\mathcal{K}\|$	DO		RO-CCG					RS-CCG				
				g%	T	opt%	g%	T	Im%		opt%	g%	T	Im%	
									mean	max				mean	max
R11	20	120	100	0.4	10000.1	0.0	9.7	28806.4	10.6	25.8	0.0	88.4	28819.0	49.3	81.7
R12	20	120	200	1.2	19712.7	0.0	17.6	28889.5	8.6	23.8	3.3	95.5	28513.1	37.6	62.7
R13	20	220	40	0.0	0.7	100.0	0.0	295.1	6.3	13.4	100.0	0.0	121.7	38.4	80.3
R14	20	220	100	0.0	35.1	16.7	4.5	24930.5	8.5	18.5	23.3	52.0	23668.9	47.4	74.5
R15	20	220	200	1.1	13375.0	0.0	15.2	28836.0	8.6	18.4	0.0	96.7	28813.7	37.5	75.2
Mean				0.5	8624.7	23.3	9.4	22351.5	8.5	25.8	25.3	66.5	21987.3	42.1	81.7

Results in Table 2.2 indicate that both model RO and model RS for instances of 100 or more commodities are challenging to solve, highlighting the need for future studies to enhance the solutions algorithms. However, the columns under Im% indicate that compared to the deterministic solutions obtained from model DO, the robust solutions from our RO-C&CG and RS-C&CG algorithms have significantly improved robust objective values with respect to model RO and model RS. Specifically, the improvements in the worst-case total cost and the worst-case normalized deviation from the prescribed cost target are 8.5% and 42.1% on average, and 25.8% and 81.7% at maximum, respectively. This demonstrates the benefit of the robust models in generating reliable CTSNDP solutions.

2.4. Details on Performance of Model DO

Although both the consolidation-based formulation proposed by Hewitt and Lehuédé (2023, 2025), and our formulation incorporate consolidations, the two models remain fundamentally different. The integer programming model of Hewitt and Lehuédé (2023, 2025) contains binary variables defined for all possible shipment combinations involved in consolidations across each transportation movement, the number of which can grow exponentially. In contrast, our model defines binary variables for each consolidation across each transportation movement, the number of which cannot exceed the number of commodities. As a result, the method proposed by Hewitt and Lehuédé (2023, 2025) to solve their integer programming model needs to enumerate all possible shipment combinations in advance, while the method that we propose to solve our integer programming model completely avoids such an enumeration. Moreover, in Hewitt and Lehuédé (2023, 2025), their models are tested on instances with pre-defined commodity paths, where the routing plan of each commodity was given a priori. In these cases, the consolidation enumeration process remains computationally tractable for the majority of instances. However, for many instances of the general CTSNDP considered in our study, where the commodity routing plan is not predetermined and must be decided, the required enumeration of all possible consolidations for every arc becomes computationally intractable.

To further illustrate the computational benefits of our approach, we conducted additional experiments to compare the computational performance of the consolidation-based formulation and our consolidation-indexed formulation on deterministic instances, including the 360 deterministic CTSNDP instances generated in our study, and the 560 instances of the deterministic Freight Transportation Network Scheduling Problem with predetermined commodity paths (FTNSP) generated by Hewitt and Lehuédé (2025).

2.4.1. Results on Deterministic CTSNDP Instances We first conducted additional computational experiments to compare the solution performance of the consolidation-based formulation and our consolidation-indexed formulation on the deterministic CTSNDP instances.

Since the consolidation-based formulation of Hewitt and Lehuédé (2023) is designed for the scheduled SNDP with pre-defined commodity paths, it cannot be directly applied to the general CTSNDP considered in our study. Therefore, we need to first extend the consolidation-based formulation of Hewitt and Lehuédé (2023) as follows to the deterministic CTSNDP by integrating routing plan decisions and holding costs. Let Ω_{ij} define the set of possible shipment consolidations on arc $(i,j) \in \mathcal{A}$, where each element represents a subset of commodities. For each $(i,j) \in \mathcal{A}$, let ϕ_ω^k indicate whether commodity k is contained in the consolidation ω, and let q_ω define the number of vehicles needed to transport consolidation $\omega \in \Omega_{ij}$ where $q_\omega = \lceil \frac{\sum_{k\in\omega} q^k}{u_{ij}} \rceil$. Given this notation, and similar to the approach in Hewitt and Lehuédé (2023), we define the following decision variables: $\delta_\omega \in \{0,1\}$ is a binary variable indicating whether consolidation ω is chosen; $y_{ij} \in \mathbb{Z}_{\geq 0}$ is a non-negative integer variable for each $(i,j) \in \mathcal{A}$, indicating the number of vehicles required by all consolidations on arc (i,j); and finally, $v_{ij}^k \in \mathbb{R}_{\geq 0}$ is a non-negative continuous variable for each $(i,j) \in \mathcal{A}$ and $k \in \mathcal{K}$, which indicates the time when commodity k departs from node i when passing through arc (i,j). To represent the routing plan decisions and holding costs, similar to our consolidation-indexed model, we introduce two additional variables: a binary variable $x_{ij}^k \in \{0,1\}$ for each $(i,j) \in \mathcal{A}$ and $k \in \mathcal{K}$, which indicates whether commodity k passes through arc (i,j); and a non-negative continuous variable $w_i^k \in \mathbb{R}_{\geq 0}$ for $i \in \mathcal{N}$ and $k \in \mathcal{K}$, which represents the holding time for commodity k at terminal i.

Accordingly, we can extend the formulation of Hewitt and Lehuédé (2023) to obtain the consolidation-based formulation for the deterministic CTSNDP as follows, which is referred to as model MHLF2023_DO:

$$\text{[MHLF2023\_DO]} \quad \min \sum_{(i,j)\in\mathcal{A}} f_{ij} \cdot y_{ij} + \sum_{k\in\mathcal{K}} \sum_{(i,j)\in\mathcal{A}} (c_{ij}^k q^k) \cdot x_{ij}^k + \sum_{k\in\mathcal{K}} \sum_{i\in\mathcal{N}} (h^k q^k) \cdot w_i^k \tag{2.1}$$

$$\text{s.t.} \sum_{(i,j)\in\mathcal{A}} x_{ij}^k - \sum_{(j,i)\in\mathcal{A}} x_{ji}^k = \begin{cases} 1, & i = o^k, \\ -1, & i = d^k, \\ 0, & \text{otherwise}, \end{cases} \quad \forall k \in \mathcal{K}, i \in \mathcal{N}, \tag{2.2}$$

$$\sum_{\omega\in\Omega_{ij}} q_\omega \delta_\omega \leq y_{ij}, \quad \forall\ (i,j) \in \mathcal{A}, \tag{2.3}$$

$$\sum_{\omega\in\Omega_{ij}} \phi_\omega^k \delta_\omega = x_{ij}^k, \quad \forall\ (i,j) \in \mathcal{A}, k \in \mathcal{K}, \tag{2.4}$$

$$\sum_{j:(j,i)\in\mathcal{A}} (v_{ji}^k + \tau_{ji} x_{ji}^k) \leq \sum_{j:(i,j)\in\mathcal{A}} v_{ij}^k, \quad \forall\ i \in \mathcal{N} \setminus \{o^k, d^k\}, k \in \mathcal{K}, \tag{2.5}$$

$$\sum_{j:(o^k,j)\in\mathcal{A}} v^k_{o^k j} \geq e^k, \quad \forall\ k \in \mathcal{K}, \tag{2.6}$$

$$\sum_{j:(j,d^k)\in\mathcal{A}} (v^k_{jd^k} + \tau_{jd^k} x^k_{jd^k}) \leq l^k, \quad \forall\ k \in \mathcal{K}, \tag{2.7}$$

$$v^k_{ij} - v^{k'}_{ij} \leq T(1 - \sum_{\omega\in\Omega_{ij}} \phi^k_\omega \phi^{k'}_\omega \delta_\omega), \quad \forall (i,j) \in \mathcal{A}, k, k' \in \mathcal{K}, \tag{2.8}$$

$$w^k_i = \begin{cases} \sum\limits_{j:(i,j)\in\mathcal{A}} v^k_{ij} - e^k, & i = o^k, \\ l^k - \sum\limits_{j:(j,i)\in\mathcal{A}} (v^k_{ji} + \tau_{ji} x^k_{ji}), & i = d^k, \quad \forall\ i \in \mathcal{N}, \forall\ k \in \mathcal{K}, \\ \sum\limits_{j:(i,j)\in\mathcal{A}} v^k_{ij} - \sum\limits_{j:(j,i)\in\mathcal{A}} (v^k_{ji} + \tau_{ji} x^k_{ji}), & \text{otherwise}, \end{cases} \tag{2.9}$$

$$x^k_{ij} \in \{0,1\}, \quad \forall\ (i,j) \in \mathcal{A}, k \in \mathcal{K}, \tag{2.10}$$

$$y_{ij} \in \mathbb{N}_{\geq 0}, \quad \forall\ (i,j) \in \mathcal{A}, \tag{2.11}$$

$$\delta_\omega \in \{0,1\}, \quad \forall\ (i,j) \in \mathcal{A}, \omega \in \Omega_{ij}, \tag{2.12}$$

$$v^k_{ij} \geq 0, \quad \forall\ (i,j) \in \mathcal{A}, k \in \mathcal{K}, \tag{2.13}$$

$$w^k_i \geq 0, \quad \forall\ i \in \mathcal{N}, k \in \mathcal{K}. \tag{2.14}$$

The objective function (2.1) indicates the total cost, including the fixed cost, flow cost, and holding cost, to be minimized. constraints (2.3)-(2.8) are extended from the consolidation-based model presented in Hewitt and Lehuédé (2023), while constraints (2.2) and (2.9) are additional constraints required by the general CTSNDP, enforcing flow balance and holding time calculations, respectively. Specifically, constraint (2.3) ensures that a sufficient number of vehicles are dispatched for each physical transportation move, based on the specific consolidations chosen for that move. Constraints (2.4) ensure that for every arc passed by a commodity, a consolidation containing that specific commodity is selected. Constraints (2.5)–(2.7) are imposed on commodities' departure times with respect to the travel time of each arc, as well as the earliest available time and the due time of each commodity. Constraints (2.8) ensure that all pairs of shipments included in a chosen consolidation for a physical transportation move depart simultaneously, where T is a significant large constant. Moreover, constraints (2.10)-(2.14) define the domains of all the decision variables.

We note that to solve model MHLF2023_DO, it needs to compute each shipment consolidation set Ω_{ij} in advance, whereas this step is not required for model DO. To improve the efficiency of solving the model from Hewitt and Lehuédé (2023), we implement the valid cuts proposed in their work. To further tighten both model MHLF2023_DO and model DO, we remove redundant $\boldsymbol{x}$, $\boldsymbol{v}$, and $\boldsymbol{s}$ variables that result from time window violations. Additionally, we apply the asymmetric representatives strategy, which is widely used in the graph coloring literature (Campêlo et al. 2008,

Malaguti et al. 2009), to effectively break solution symmetry and enhance tractability for model DO. Both models are solved using the Gurobi solver (v.10.0.2), with an optimality gap of 1% and a time limit of one hour, which are common for solving deterministic CTSNDP instances.

The computational results on deterministic CTSNDP instance are presented in Table 2.3 below. For each model, we report the percentage of instances solved to optimality in column "opt%", the average optimality gap in column "gap%", the average computational time in CPU seconds in column "time", and the percentage of instances where the consolidation enumeration could not be completed within the time limit in column "no_MIP" (for these instances, the final gap is set to 100%). Define $\mathcal{K}_{ij}$ as the set of commodities k can pass arc $(i,j) \in \mathcal{A}$ without violating the time constraints. The consolidation-based formulation proposed by Hewitt and Lehuédé (2023) required to enumerate all possible combinations from $\mathcal{K}_{ij}$ for all $(i,j) \in \mathcal{A}$. The enumeration complexity increases along with the increase of $|\mathcal{K}_{ij}|$. The maximum and minimize value of $\mathrm{K} = \max\{|\mathcal{K}_{ij}| : (i,j) \in \mathcal{A}\}$ for each instance class are presented in columns "max K" and "min K", serving as an indicator of enumeration complexity of each instance class.

Table 2.3 Computational results of MHLF2023_DO and DO on CTSNDP instances.

Class	max K	min K	MHLF2023_DO				DO		
			opt%	no_MIP	gap%	time	opt%	gap%	time
R4	3	2	100%	0.0%	0.2%	0.0	100%	0.1%	0.0
R5	8	5	100%	0.0%	0.3%	0.1	100%	0.4%	0.1
R6	18	7	100%	0.0%	0.5%	0.5	100%	0.6%	0.4
R7	5	4	100%	0.0%	0.2%	0.1	100%	0.2%	0.1
R8	8	7	100%	0.0%	0.3%	0.2	100%	0.4%	0.1
R9	18	9	100%	0.0%	0.4%	0.4	100%	0.5%	0.3
R10	10	5	100%	0.0%	0.4%	0.5	100%	0.5%	0.3
R11	41	23	50%	50.0%	50.4%	1816.9	83%	1.3%	716.2
R12	69	49	0%	100.0%	100.0%	3600.1	63%	2.0%	1421.6
R13	19	11	100%	0.0%	0.5%	1.2	100%	0.5%	0.6
R14	29	22	100%	0.0%	0.7%	145.8	100%	0.8%	7.6
R15	49	27	50%	50.0%	50.4%	2223.8	70%	2.0%	1139.8

The results in Table 2.3 show that for instances with a small number of commodities per arc ("max K" less than 20), both the consolidation-based formulation (MHLF2023_DO) extended from Hewitt and Lehuédé (2023) and our consolidation-indexed formulation (DO) can be efficiently to optimality. For these instances, the performance of the two models is comparable.

For instances with a large number of commodities per arc ("min K" larger than 20), our consolidation-indexed formulation (DO) performs significantly better than the consolidation-based formulation (MHLF2023_DO) extended from Hewitt and Lehuédé (2023). Specifically, for instances

in class R14, both models can be solved to optimality within the time limit, but our model requires about 94% less computational time. For instances in classes R11, R12, and R15, a large proportion fail to complete the precomputation of shipment consolidation sets Ω_{ij} for model MHLF2023_DO within the time limit. In contrast, our model DO can be solved to optimality for many more instances and achieves an average optimality gap of less than 2% across all these instance classes.

2.4.2. Results on FTNSP Instances We also conducted additional experiments to compare the performance of our consolidation-indexed formulation against the consolidation-based formulation and its column generation algorithm proposed by Hewitt and Lehuédé (2025) over their instances of the Freight Transportation Network Scheduling Problem (FTNSP).

Since the FTNSP involves predefined commodity routing and does not include holding costs, we need to adapt our consolidation-indexed formulation accordingly, for which the variables and associated constraints related to routing plan decisions and holding costs need to be removed. Consider the delivery path $p^k = \{v_1^k = o^k, ..., v_{|p^k|^k} = d^k\}$ of each commodity $k \in \mathcal{K}$ given in the FTNSP. For each commodity $k \in \mathcal{K}$, we let the node set $\mathcal{N}^k \subseteq \mathcal{N}$ contain the nodes in the path p^k and the arc set $\mathcal{A}^k \subseteq \mathcal{A}$ contain the arcs (v_i^k, v_{i+1}^k) in the path p^k. We also let $\mathcal{K}_{ij} = \{k \in \mathcal{K} : (i,j) \in \mathcal{A}^k\}$ denote the set of commodities with a path that contains arc $(i,j) \in \mathcal{A}$. We note that given the commodity path p^k, along with the earliest available time e^k and latest due time l^k for commodity k, one can derive a time window $[\alpha_i^k, \beta_i^k]$ during which commodity k can depart from each node i in its path. Define $\bar{\alpha}_{ij} = \min\{\alpha_i^k : k \in \mathcal{K}_{ij}\}$ and $\bar{\beta}_{ij} = \max\{\beta_i^k : k \in \mathcal{K}_{ij}\}$. With the same decision variables $\boldsymbol{z}$, $\boldsymbol{y}$, $\boldsymbol{v}$, and $\boldsymbol{b}$, we can obtain the following consolidation-indexed formulation for the FTNSP, denoted as FTNSP_DO:

$$\min \sum_{(i,j)\in\mathcal{A}} \sum_{r=1}^{|\mathcal{K}_{ij}|} f_{ij} \cdot y_{ijr} \tag{2.15}$$

$$\text{s.t.} \sum_{k\in\mathcal{K}_{ij}} q^k z_{ijr}^k \le u_{ij} y_{ijr}, \quad \forall\ (i,j) \in \mathcal{A}, r \in \{1,2,...,|\mathcal{K}_{ij}|\}, \tag{2.16}$$

$$\sum_{r=1}^{|\mathcal{K}_{ij}|} z_{ijr}^k = 1, \quad \forall\ k \in \mathcal{K}, (i,j) \in \mathcal{A}^k, \tag{2.17}$$

$$\sum_{j:(j,i)\in\mathcal{A}^k} (v_{ji}^k + \tau_{ji}) \le \sum_{j:(i,j)\in\mathcal{A}^k} v_{ij}^k, \quad \forall\ k \in \mathcal{K}, i \in \mathcal{N}^k \setminus \{o^k, d^k\}, \tag{2.18}$$

$$\sum_{j:(o^k,j)\in\mathcal{A}^k} v_{o^k j}^k \ge e^k, \quad \forall\ k \in \mathcal{K}, \tag{2.19}$$

$$\sum_{j:(j,d^k)\in\mathcal{A}^k} (v_{jd^k}^k + \tau_{jd^k}) \le l^k, \quad \forall\ k \in \mathcal{K}, \tag{2.20}$$

$$v_{ij}^k \le b_{ijr} + M(1 - z_{ijr}^k), \quad \forall\ k \in \mathcal{K}, (i,j) \in \mathcal{A}^k, r \in \{1,2,...,|\mathcal{K}_{ij}|\}, \tag{2.21}$$

$$v_{ij}^k \geq b_{ijr} - M(1 - z_{ijr}^k), \quad \forall\ k \in \mathcal{K}, (i,j) \in \mathcal{A}^k, r \in \{1,2,...,|\mathcal{K}_{ij}|\}, \tag{2.22}$$

$$y_{ijr} \in \mathbb{N}_{\geq 0}, \quad \forall\ (i,j) \in \mathcal{A}, r \in \{1,2,...,|\mathcal{K}_{ij}|\}, \tag{2.23}$$

$$z_{ijr}^k \in \{0,1\}, \quad \forall\ k \in \mathcal{K}, (i,j) \in \mathcal{A}^k, r \in \{1,2,...,|\mathcal{K}_{ij}|\}, \tag{2.24}$$

$$\alpha_i^k \leq v_{ij}^k \leq \beta_i^k, \quad \forall\ k \in \mathcal{K}, (i,j) \in \mathcal{A}^k, \tag{2.25}$$

$$\bar{\alpha}_{ij} \leq b_{ijr} \leq \bar{\beta}_{ij}, \quad \forall\ (i,j) \in \mathcal{A}, r \in \{1,2,...,|\mathcal{K}_{ij}|\}. \tag{2.26}$$

The objective (2.16) seeks to minimize the total fixed cost. Constraints (2.16) are capacity constraints. Constraints (2.17) are consolidation coverage constraints, ensuring that for every arc (i,j) on the flat path of commodity $k \in \mathcal{K}$, there exists a consolidation of arc (i,j) that contains k. Constraints (2.18)–(2.20) are imposed on commodities' departure times with respect to the travel time of each arc, as well as the earliest available time and the due time of each commodity. Constraints (2.21) and (2.22) ensure that for each arc $(i,j) \in \mathcal{A}$, the commodities that are consolidated to be shipped together through (i,j) have the same departure time from node i. Constraints (2.23)-(2.26) define the domains of all the decision variables.

To further tighten model FTNSP_DO, we utilize the asymmetric representatives strategy, which is widely adopted in the graph coloring literature(Campêlo et al. 2008, Malaguti et al. 2009). The key idea of the asymmetric representatives strategy is to sort the commodities for each arc based on the maximum size of their conflict subset, and associate a representative commodity with each consolidation, enforcing that the r'-th commodity can be included in the r-th consolidation only if $r' \leq r$ and the representative commodity of the r-th consolidation is also assigned to it. Therefore, the model can be further enhanced by incorporating the following valid inequalities:

$$y_{ijr} \geq \left\lceil \frac{q^{k_{ijr}}}{u_{ij}} \right\rceil z_{ijr}^{k_{ijr}}, \quad \forall (i,j) \in \mathcal{A}, r \in \{1,2,...,|\mathcal{K}_{ij}|\}, \tag{2.27}$$

$$\sum_{r=1}^{|\mathcal{K}_{ij}|} y_{ijr} \geq \underline{y}_{ij}, \quad \forall (i,j) \in \mathcal{A}, \tag{2.28}$$

where k_{ijr} is the r-th commodity in $\mathcal{K}_{ij}$ and $\underline{y}_{ij}$ is the lower bound on the number of vehicles required to serve all commodities in $\mathcal{K}_{ij}$. We know that $\underline{y}_{ij} \geq \lceil \sum_{k \in \mathcal{K}_{ij}} q^k / u_{ij} \rceil$, and the value of this lower bound $\underline{y}_{ij}$ can be obtained by solving a graph coloring problem for each arc (i,j).

For each FTNSP instance from Hewitt and Lehuédé (2025), we solve our model FTNSP_DO using the Gurobi solver (v.10.0.2), with an optimality tolerance of 1% and a time limit of two hours, consistent with the settings in Hewitt and Lehuédé (2025). All experiments were conducted on an Intel(R) Core(TM) i7-8700 desktop PC (3.20 GHz, 64 GB RAM). We compared our results with those obtained by the two solution methods presented in Hewitt and Lehuédé (2025): a static method, which directly uses an optimization solver and is denoted as *Cons-FINSP*($\mathcal{C}$), and

a dynamic method, which is based on column generation and denoted as *IP-ColGen*. Both of these two benchmark methods are based on the consolidation-based formulation.

Table 2.4 presents the computational results, reporting the average percentage of instances solved to optimality and the average running time across all instances. The results for *Cons-FINSP*($\mathcal{C}$) and *IP-ColGen* are taken directly from Hewitt and Lehuédé (2025).

The results in Table 2.4 show that our consolidation-indexed formulation solves all the FTNSP instances to optimality in less than 11 seconds on average, significantly outperforming both the consolidation-based formulation and its column generation-based algorithm. This demonstrates that, although the primary focus of our study is not on solving the deterministic problem, our new consolidation-indexed formulation also advances the literature on deterministic freight transportation network scheduling problems.

Table 2.4 Computational results on FTNSP Instances of Hewitt and Lehuédé (2025).

Method	Percentage solved (%)	Time (s)
Cons-FINSP($\mathcal{C}$)	89.29	354.27
IP-ColGen	91.96	189.37
FTNSP_DO	100.00	10.89

References

Boland, N., Hewitt, M., Marshall, L., Savelsbergh, M., 2017. The continuous-time service network design problem. Operations Research 65, 1303–1321.

Campêlo, M., Campos, V.A., Corrêa, R.C., 2008. On the asymmetric representatives formulation for the vertex coloring problem. Discrete Applied Mathematics 156, 1097–1111.

Crainic, T.G., Fu, X., Gendreau, M., Rei, W., Wallace, S.W., 2011. Progressive hedging-based metaheuristics for stochastic network design. Networks 58, 114–124.

Ghamlouche, I., Crainic, T.G., Gendreau, M., 2003. Cycle-based neighbourhoods for fixed-charge capacitated multicommodity network design. Operations Research 51, 655–667.

Hewitt, M., Lehuédé, F., 2023. New formulations for the scheduled service network design problem. Transportation Research Part B: Methodological 172, 117–133.

Hewitt, M., Lehuédé, F., 2025. The freight transportation network scheduling problem: An integer programming-based column generation algorithm. INFORMS Journal on Computing URL: `https://pubsonline.informs.org/doi/abs/10.1287/ijoc.2023.0435`.

Lanza, G., Crainic, T.G., Rei, W., Ricciardi, N., 2021. Scheduled service network design with quality targets and stochastic travel times. European Journal of Operational Research 288, 30–46.

Malaguti, E., Monaci, M., Toth, P., 2009. Models and heuristic algorithms for a weighted vertex coloring problem. Journal of Heuristics 15, 503–526.

Sarayloo, F., Crainic, T.G., Rei, W., 2021a. A learning-based matheuristic for stochastic multicommodity network design. INFORMS Journal on Computing 33, 643–656.

Sarayloo, F., Crainic, T.G., Rei, W., 2021b. A reduced cost-based restriction and refinement matheuristic for stochastic network design problem. Journal of Heuristics 27, 325–351.

Wang, Z., Qi, M., 2020. Robust service network design under demand uncertainty. Transportation Science 54, 676–689.